Carcinogenesis vol.32 no.3 pp.305–311, 2011
doi:10.1093/carcin/bgq272
Advance Access publication December 16, 2010

High frequency of *TTK* mutations in microsatellite-unstable colorectal cancer and evaluation of their effect on spindle assembly checkpoint

Iina Niittymäki, Alexandra Gylfe, Leena Laine[1], Marko Laakso[2], Heli J.Lehtonen, Johanna Kondelin, Jaana Tolvanen, Kari Nousiainen[2], Jeroen Pouwels[1], Heikki Järvinen[3], Kyösti Nuorva[4], Jukka-Pekka Mecklin[5], Markus Mäkinen[6], Ari Ristimäki[7], Torben F.Ørntoft[8], Sampsa Hautaniemi[2], Auli Karhu, Marko J.Kallio[1] and Lauri A.Aaltonen*

Department of Medical Genetics, Genome-Scale Biology Research Program, Biomedicum Helsinki, PO Box 63, FIN-00014, University of Helsinki, Finland, [1]Medical Biotechnology, VTT Technical Research Center of Finland, Turku, Finland, [2]Computational Systems Biology Laboratory, Institute of Biomedicine and Genome-Scale Biology Research Program, Biomedicum Helsinki, University of Helsinki, Finland, [3]Department of Surgery, Helsinki University Hospital, Helsinki FIN-00029, Finland, [4]Department of Pathology and [5]Department of Surgery, Jyväskylä Central Hospital, Jyväskylä FIN-40620, Finland, [6]Department of Pathology, Oulu University Hospital, Oulu FIN-90014, Finland, [7]Department of Pathology, HUSLAB and Haartman Institute and Genome-Scale Biology Research Program, Helsinki University Central Hospital and University of Helsinki, Helsinki FIN-00014, Finland and [8]Molecular Diagnostic Laboratory, Department of Clinical Biochemistry, Aarhus University Hospital, Aarhus DK8200, Denmark

*To whom correspondence should be addressed.
Tel: +358 9 19125595; Fax: +358 9 19125105;
Email: lauri.aaltonen@helsinki.fi

Frameshift mutations frequently accumulate in microsatellite-unstable colorectal cancers (MSI CRCs) typically leading to down-regulation of the target genes due to nonsense-mediated messenger RNA decay. However, frameshift mutations that occur in the 3′ end of the coding regions can escape decay, which has largely been ignored in previous works. In this study, we characterized non-sense-mediated decay-escaping frameshift mutations in MSI CRC in an unbiased, genome wide manner. Combining bioinformatic search with expression profiling, we identified genes that were predicted to escape decay after a deletion in a microsatellite repeat. These repeats, located in 258 genes, were initially sequenced in 30 MSI CRC samples. The mitotic checkpoint kinase *TTK* was found to harbor decay-escaping heterozygous mutations in exon 22 in 59% (105/179) of MSI CRCs, which is notably more than previously reported. Additional novel deletions were found in exon 5, raising the mutation frequency to 66%. The exon 22 of *TTK* contains an A_9–G_4–A_7 locus, in which the most common mutation was a mononucleotide deletion in the A_9 (c.2560delA). When compared with identical non-coding repeats, *TTK* was found to be mutated significantly more often than expected without selective advantage. Since TTK inhibition is known to induce override of the mitotic spindle assembly checkpoint (SAC), we challenged mutated cancer cells with the microtubule-stabilizing drug paclitaxel. No evidence of checkpoint weakening was observed. As a conclusion, heterozygous *TTK* mutations occur at a high frequency in MSI CRCs. Unexpectedly, the plausible selective advantage in tumourigenesis does not appear to be related to SAC.

Introduction

Around 15% of all colorectal cancers (CRCs), including those associated with Lynch syndrome, develop through the microsatellite instability (MSI) pathway (1–3). MSI tumourigenesis is driven by a defective mismatch repair system that in Lynch syndrome is caused by germ line mutations in the mismatch repair genes (most commonly in *MLH1* and *MSH2*) and in sporadic MSI CRC typically by the epigenetic silencing of *MLH1* (4). The genetic and clinicopathologic profile of MSI CRC differs from the main subtype of CRC, known as microsatellite stable (MSS) or chromosomal instability type, yet these pathways are partially overlapping (5). MSI cells usually have a fairly normal diploid karyotype but instead are prone to accumulate point mutations as well as deletions and insertions at microsatellite repeats. These short repetitive sequences are dispersed all over the genome at both non-coding and coding areas. Whenever a frameshift mutation randomly targets a crucial gene, it might provide the cell with growth advantage and be selected for in tumourigenesis, manifesting as a high mutation frequency in MSI cancers. The best-established target gene with robust functional evidence is *TGFBR2* that is inactivated in the majority of MSI CRCs (6).

Frameshift mutations typically lead to premature termination codons (PTCs) and truncated peptides, which is why most of the target mutations are assumed to have loss of function effects. The PTC-containing messenger RNAs (mRNAs) are usually degraded by nonsense-mediated messenger RNA decay (NMD), which prevents the translation of aberrant transcripts (7). During splicing, the exon–exon junctions associate with a protein complex that signals the position of excised introns to the translational machinery. Since the correct stop codon is located in the end of the last exon, translating ribosomes are stalled on recognising a PTC upstream of an exon junction complex and consequently the mRNA is committed to decay. However, when the PTC locates in the last exon or after 55 nucleotides upstream of the most 3′ exon–exon junction, it is usually missed by the NMD machinery (8). Some of the frequently mutated mRNAs, such as *BAX* and *TCF-4*, are indeed expressed in MSI CRC cell lines (9). Of the dozens of published MSI target genes, only few seem to have dominant-negative or oncogenic effects, rather than being tumour suppressors. In *TCF-4*, a frameshift mutation in the last exon decreases the protein's ability to interact with a repressor, enhancing *TCF-4* transcriptional activity and Wnt signaling (10).

Reduced expression has been utilized in the search for MSI target genes in previous studies focusing on identification of MSI CRC suppressor genes (11,12). In this study, we aimed at identifying oncogenic NMD-escaping frameshift mutations in MSI CRC, from genes overexpressed in this tumour type. The mitotic spindle assembly checkpoint (SAC) kinase *TTK* (*Dual-specificity protein kinase TTK*, also known as *Monopolar spindle 1*, *MPS1*) was found to harbor NMD-escaping frameshift mutations in 59% of MSI CRCs. Interference with TTK function leads to chromosome missegregation in cancer cells, and when treated with the microtubule-stabilizing drug paclitaxel (taxol), it causes weakening of the drug-induced SAC (13–15). Here, we found no evidence of checkpoint override in heterozygously mutated cancer cells when treated with paclitaxel, suggesting that the mutation is not sufficient to dysregulate SAC in the presence of one intact allele.

Abbreviations: cDNA, complementary DNA; CRC, colorectal cancer; GFP, green fluorescent protein; mRNA, messenger RNA; MSI, microsatellite instability; MSI CRC, microsatellite-unstable colorectal cancer; MSS, microsatellite stable; NMD, nonsense-mediated messenger RNA decay; PCR, polymerase chain reaction; PTC, premature termination codon.

Materials and methods

Patient samples

A population-based sample series of 1042 colorectal adenocarcinomas, which has been previously characterized elsewhere, was used in the study (16,17). The samples were collected between 1994 and 1998 from nine Finnish central hospitals. Additional samples were chosen from another CRC sample series collected since 1998. In short, DNA was extracted with standard methods from fresh-frozen tumour and corresponding normal tissue or blood. Comprehensive

data obtained from registries and from pathologist's evaluation were available from all the patients. The MSI status of the tumours was previously determined and all the tumours showing MSI were screened for mutations in *MLH1* and *MSH2* genes, in order to identify potential Lynch syndrome patients. The 30 MSI CRCs used in the initial sequencing effort consisted of 20 randomly selected sporadic and 10 Lynch syndrome associated MSI CRCs. In the extended set of 100 MSI CRCs, there were altogether 23 Lynch syndrome associated samples. An additional set of 31 MSI CRC DNAs extracted from paraffin-embedded tumours from Northern Finland was available for the analysis of clinicopathologic associations. All the samples were obtained with informed consent and Ethical Review Board approval.

Cell lines and culture conditions

MSI CRC cell lines VACO5, CCL-231, GP5D, HCA7, HCT8, HCT15, HCT116, LIM1215, LoVo, LS174T, LS180, RKO, SNUC2B and DLD1, cervical carcinoma cell line HeLa and human embryonic kidney cell line HEK293 were purchased from the American Type Culture Collection (Manassas, VA) or the European Collection of Cell Cultures (Salisbury, UK) or provided by Dr Ian Tomlinson. Cells were maintained in their recommended media supplemented with penicillin/streptomycin, glutamine and 10% fetal bovine serum.

Bioinformatic search for repeat-containing genes

A frameshift predictor software was created to search all protein-coding transcripts from the Ensembl database (Homo sapiens 45_36g; www.ensembl.org) that contained coding mononucleotide repeats from 6 to 10 bp and were anticipated to escape NMD after one nucleotide deletion in the repeat. Based on the literature, NMD escape was assumed to occur if the frameshift-induced termination codon located in the C-terminal part of the gene, that is, after 55 bp upstream from the last exon–exon junction or anywhere in the last exon.

Expression microarray analysis

A previously characterized expression array dataset was available for this study (18). In brief, RNA samples from 72 MSI CRCs and 10 normal colonic mucosas were analyzed with Human Genome U133 Plus 2.0 Array (Affymetrix, Santa Clara, CA). Ensembl probe sequence annotations (Hs133P_Hs_ENSG) were obtained from Bioconductor (http://www.bioconductor.org/), and the expression values were called for the robust multi-array analysis normalized arrays. Differentially expressed genes were obtained by selecting genes with a mean fold change of two between cases and controls. The gene set was further limited by calculating *T*-test statistics for all genes and by applying robust false discovery rate correction for multiple testing for the obtained *P*-values (19). Genes with q-value <0.05 were selected for further analysis.

Mutation detection by genomic sequencing

Human genomic reference sequences were downloaded from the Ensembl database (releases 46 August 2007 to 50 July 2008; http://www.ensembl.org/) and polymerase chain reaction (PCR) primers were designed with Primer3 software (http://frodo.wi.mit.edu/primer3/). Genomic DNA extracted from fresh-frozen primary tumours and commercial cell lines was amplified with PCR using either AmpliTaq Gold DNA polymerase (Applied Biosystems, Foster City, CA) for the repeats of 6–7 bp or Phusion DNA polymerase (Finnzymes, Espoo, Finland) for the repeats of 8–10 bp. PCR products were sequenced using Applied Biosystems BigDye v3.1 sequencing chemistry and ABI3730 automatic DNA sequencer. Sequencing graphs were analyzed with Mutation Surveyor (SoftGenetics, State College, PA) and Chromas (http://www.technelysium.com.au/) softwares. A heterozygous change in the sequencing graph was scored as a mutation if the mutant peak height was 15% or more of the wild-type peak height. The PCR and sequencing was repeated whenever a mutation was encountered. The somatic origin of the mutation was confirmed by sequencing the respective germ line DNA. Of the paraffin-embedded tumour samples, only those were included in the analysis from which unambiguous sequencing results were obtained after several reruns.

Cloning and sequencing of TTK from a primary tumour

Total RNA was extracted with TRIzol reagent (Invitrogen, Carlsbad, CA) from a fresh-frozen tumour tissue. RNA was reverse transcribed to complementary DNA (cDNA) with M-MLV enzyme (Promega, Madison, WI). The cDNA was amplified with Phusion DNA polymeraseand ligated into a Zero Blunt PCR Cloning Kit vector (Invitrogen). TOP10 *Escherichia coli* bacteria were transformed with the ligation and colonies were selected for plasmid DNA extraction and sequencing. Plasmids were extracted with Nucleo Spin Extraction Kit (Clontech Laboratories, Mountain View, CA) and sequenced using Applied Biosystems BigDye v3.1 sequencing chemistry and ABI3730 automatic DNA sequencer.

Laser capture microdissection

Fresh-frozen tumour sections (10 μm) were prepared, dehydrated and stained with HistoGene LCM Frozen Section Staining Kit (Arcturus, Mountain View, CA). An additional hematoxylin-eosin staining was carried out for sections from each tumour and the presence of malignant epithelial tissue was confirmed beforehand with microscopy. Laser capture microdissection was performed with Arcturus Microdissection Instrument on CapSure laser capture microdissection Caps (Arcturus). PicoPure DNA Extraction Kit (Arcturus) was used to extract genomic DNA from the caps.

Western blot analysis

Total cellular protein was extracted from cultured cell lines with radioimmunoprecipitation assay buffer (Pierce, Rockford, IL) supplemented with protease inhibitor cocktail (Roche Diagnostics, Mannheim, Germany). Twenty-five micrograms of each total protein was fractionated by sodium dodecyl sulfate–polyacrylamide gel electrophoresis in a 7.5% Tris–HCl polyacrylamide gel and transferred to a nitrocellulose filter. Immunoblots were incubated overnight at 4°C with a primary mouse monoclonal antibody against TTK N-terminus (H00007272-M01; Abnova, Taipei City, Taiwan) at a dilution of 1:500 in 5% milk powder in phosphate-buffered saline buffer. An appropriate secondary antibody was incubated at room temperature for 1 h. Immunoblots were visualized with enhanced chemiluminescence Plus western blot detection system (Amersham Biosciences/GE Healthcare, London, UK). A primary antibody against alpha-tubulin was used as a loading control in an identical separate sodium dodecyl sulfate–polyacrylamide gel electrophoresis. Western blot of HEK293 cells transfected with pE green fluorescent protein (GFP)-TTK expression constructs was performed using the same antibodies in one 10% gel. Proteins were extracted 30 h post-transfection.

Immunohistochemistry

Paraffin-embedded tumour sections were immunohistochemically stained with a mouse monoclonal antibody against the N-terminus of human TTK (catalog no. 35-9100; Zymed Laboratories, Invitrogen). Tris–ethylenediaminetetraacetic acid buffer (pH 9) was used in heat-induced epitope retrieval. The slides were incubated in an antibody dilution of 1:50 for 2 h. Detection was performed with anti-Mouse/Rabbit PowerVision Poly-HRP IHC Detection System (Leica Biosystems Newcastle Ltd, Newcastle, UK). Images were acquired with Leica DM LB microscope (Meyer Instruments, Houston, TX), Olympus DP50 camera and Studio Lite software.

Expression construct, transient transfection and fluorescence microscopy

Wild-type and mutant (c.2560delA) *TTK* cDNAs were cloned into pEGFP-C2 Vector (Clontech Laboratories) in which the GFP tag locates N-terminally to the gene. HEK293 cells were transfected with the plasmids using Lipofectamine2000 reagent (Invitrogen) according to manufacturer's instructions. Paclitaxel (Molecular Probes, Sunnyvale, CA) was added at 20 nM concentration 24 h post-transfection and the cells were fixed with 2% paraformaldehyde 30 h post-transfection. DNA was stained with 4′,6-diamidino-2-phenylindole (Molecular Probes) at 0.1 μg/ml in H_2O. Fixed cells were examined with fluorescence microscopy using Zeiss Axiovert 200M microscope and MetaMorph software (Universal Imaging, Buckinghamshire, UK). Z-stack images were acquired with ×63 objective using 0.3 μm step size.

Live-cell imaging

LoVo (80×10^3 cells per well), HCT116 (35×10^3 cells per well), DLD1 (35×10^3 cells per well) and HCT8 (50×10^3 cells per well) cells were grown on 48-well plates and filmed once per hour for 96 h with IncuCyte live-cell imaging system (Essen Instruments, Ann Arbor, MI). Paclitaxel was added after 21 h of incubation at 10, 25 and 50 nM concentrations. Dimethyl sulfoxide was used as a negative control. The experiment was performed twice.

Colony formation assay

LoVo, HCT116, DLD1 and HCT8 cells were grown on 12-well plates at a confluence of 500, 2500 and 10×10^3 cells per well. Paclitaxel or dimethyl sulfoxide were added after 2 days of incubation at 1, 5, 10 and 25 nM concentrations and the drug-containing media were changed every 48 h. After 8 days of incubation, the cells were fixed with 96% methanol and stained with 0.05% Crystal Violet (Sigma–Aldrich, St Louis, MO) in H_2O for 30 min. Photographs were taken with GeneGenius bio imaging system and GeneSnap software and colonies were counted with GeneTools (all from Syngene, Cambridge, England) using same parameters for each plate. Average counts from two replicates were obtained.

Statistical methods

All the analyses were performed with R software (www.r-project.org). Pearson's chi-squared test was used to calculate differences between the mutation frequencies of *TTK* and control repeats, to evaluate the distribution of mutations in exons 5 and 22 of *TTK*, as well as in the analysis of clinicopathological associations. In the latter analysis, Bonferroni's correction for multiple testing was applied for the obtained *P*-values (data not shown in Table III).

Results

Identification of TTK as an MSI CRC target gene

A bioinformatic tool was created to search for transcripts with a 6–10 bp long mononucleotide repeat located near the 3′ end of the coding region and predicted to escape NMD after one base deletion (see Methods for details). The great majority of the frameshift mutations in MSI tumours are deletions (20), which is why insertions were not included. Altogether, 7168 mononucleotide repeats of 6–10 bp in all Ensembl transcripts were anticipated to cause NMD escape of the corresponding mRNA. In order to enhance the likelihood of identifying oncogenic mutations that are selected for in the tumours, only the overexpressed genes were chosen for analysis. Based on a previously characterized expression microarray dataset (18), 330 genes from the initial frameshift prediction list were overexpressed at least 2-fold in MSI CRC compared with normal colonic mucosa. After the exclusion of unsuitable loci, such as polymorphic and intron-overlapping repeats, 281 repeat fragments in 258 genes were successfully sequenced in 30 MSI CRCs. Whenever the mutation frequency >20%, an additional 70 MSI CRCs were analyzed. The great majority of the analyzed repeats had no mutations, and 97% (272/281) of the repeats had a mutation frequency of ≤7%. Four genes were mutated in >20% of the samples in the 100 MSI CRCs analyzed: A_9 and A_7 of *TTK* in 67%, A_{10} of *TMEM97* (*Transmembrane protein 97*) in 39%, G_8 of *ARS2* (*Arsenite-resistance protein 2*) in 33% and T_9 of *LENG8* (*Leukocyte receptor cluster member 8*) in 31%. Since MSI tumours harbor large amounts of neutral bystander changes (20), the mutation frequencies of the four genes were compared with mutation frequencies in identical control repeats located in intronic and intergenic regions. For this comparison, we used our unpublished dataset of background mutation frequencies in MSI CRC, from which cutoff frequencies had been calculated using regression analysis introduced by Woerner *et al.* (21), (Alhopuro P, Sammalkorpi S, Niittymäki I, Biström M, Raitila A, Saharinen J, Nousiainen K, Lehtonen H, Heliövaara E, Puhakka J, Tuupanen S, Sousa S, Seruca R, Ferreira AM, Hofstra RMW, Mecklin JP, Järvinen H, Ristimäki A, Ørntoft TF, Hautaniemi S, Arango D, Karhu A, Aaltonen LA, in preparation). Only *TTK* was mutated more than expected merely by chance when compared with identical control repeats and was therefore chosen for further evaluation.

TTK mutation spectrum in CRCs

The mutations in the last exon (ex22) of *TTK* were most commonly mononucleotide deletions in the A_9 (c.2560delA, ENST00000230510; Figure 1A and B). The 100 MSI CRCs and 12 genetically different MSI CRC cell lines were sequenced for the entire coding region of *TTK*. Additional frameshift mutations were observed in two A_7 repeats in exon 5, in an A_4 repeat in exon 20 and in an A_5 repeat in exon 2 (Table I). The overall frameshift mutation frequency of *TTK* in the 100 MSI CRCs was 74% and in MSI CRC cell lines 75% (9/12; Table II).

A population-based series of 1027 CRC samples, including 179 MSI and 848 MSS, was screened for *TTK* mutation hotspots in exons 22 and 5. The MSI tumours (including the 100 previously analyzed) had a mutation frequency of 59% (105/179) in exon 22. The overall mutation frequency in exons 22 and 5 was 66% (119/179; Table I). Fourteen tumours that were wild-type for exon 22 had a deletion in exon 5 (14/76), and seven tumours harbored both mutations (7/103). Exon 5 deletions were hence enriched in the exon 22 wild-type tumours ($P = 0.017$). Of the 848 sequenced MSS tumours, three had a frameshift mutation (c.2571delA in two, c.2560dupA in one) in exon 22 (3/848). None of the analyzed MSS tumours had mutations in exon 5 (0/824). Sequencing of the entire coding region of the three MSS mutants did not reveal other changes outside exon 22. Additionally, the following somatic missense mutations were identified in three MSI CRCs: R256W (c.766C>T) in exon 7, L356P (c.1067T>C) in exon 10 and R185Q (c.554G>A) in exon 5. Two novel germ line missense changes were also detected: E840K (c.2518G>A) in exon 22 in an MSS CRC and E198K (c.593G>A) in exon 5 in an MSI CRC. These changes were not analyzed further since they were not located in any known functional domains.

The A_9 and A_7 repeats in exon 22 of *TTK* originally tagged by the frameshift predictor are separated only by a G_4 repeat. Given that this locus could be more unstable than A_9 alone, the human genome was searched for identical A/T_9—G/C_4—A/T_7 control loci from intronic and intergenic regions. Seven A_9—C_4—A_7 repeats (three intronic and four

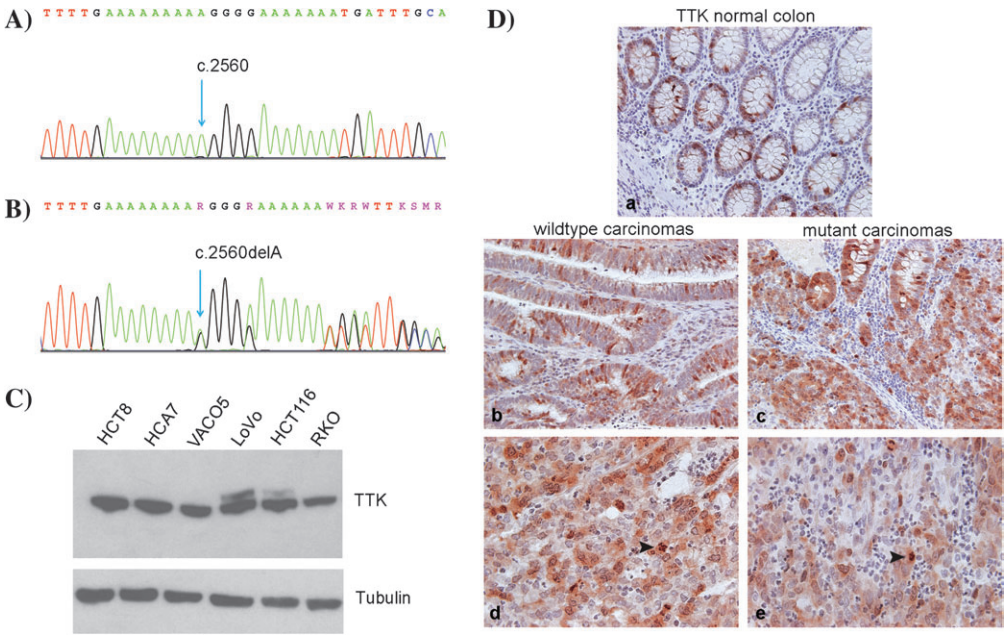

Fig. 1. Wild-type A_9-G_4-A_7 locus in the exon 22 of *TTK* in HCT8 cell line (**A**) and c.2560delA mutation in LoVo cell line. (**B**) TTK protein in MSI CRC cell lines (**C**) Elongated protein was visible in LoVo and HCT116 cell lines that have the c.2560delA mutation in exon 22. Only the normal sized (97 kDa) protein was detected in the wild-type cell lines HCT8 and VACO5 and in HCA7 and RKO that harbor mutations in exon 5 (see Table II). Immunohistochemical staining of TTK in normal colonic mucosa (**D**, a) and in four representative MSI CRCs (D, b–e). Similar expression was observed in both *TTK* wild-type cancers (b and d) and those with the c.2560delA mutation (c and e). Arrowheads point at stained chromatin of cells undergoing mitosis (d, e). Original magnifications: ×200 (a–c), ×400 (d, e).

Table I. *TTK* frameshift mutations in MSI and MSS CRC

Exon	MSI	MSS	Coding nomenclature	Translational consequence
2	1/100	nd	c.86delA	NMD-competent
5	21/179 (12%)	0/824	c.484delA, c.575delA	NMD-competent
20	1/100	nd	c.2331delA	NMD-competent
22	105/179 (59%)	3/848	c.2560delA[a]	NMD-escaping

Exon 5 and 22: 66% (119/179).
[a]The most frequent mutation, see Results for others.

Table II. *TTK* frameshift mutations in MSI CRC cell lines

Cell line	Mutation (exon)
VACO5	wt
CCL-231	c.2560delA (22)
GP5D	c.2571delA, c.2560delA (22)
HCA7	c.484delA (5)
HCT8	wt
HCT15[a]	wt
DLD1[a]	wt
HCT116	c.2560delA (22)
LIM1215	c.2560delA (22)
LoVo	c.2560delA (22)
LS174T[a]	c.484delA (5)
LS180[a]	c.484delA (5)
RKO	c.575delA, c.2559_2560delAA (5,22)
SNUC2B	c.2559_2560delAA (22)

Exon 22: 58% (7/12) and exon 5 and 22: 75% (9/12).
[a]Originally from the same primary tumour.

intergenic) were successfully sequenced in 30 MSI CRCs (see supplementary information, available at *Carcinogenesis* Online, for locations). After exclusion of germ line polymorphisms, data were gathered from 139 repeats, of which 36% were mutated (50/139). The numbers indicate that *TTK* indeed harbors mutations in its last exon significantly more than expected by chance (105/179 versus 50/139, $P = 9.5 \times 10^{-5}$). When taking into account only the mutations involving A_9 (and not G_4 or A_7), the difference was similar (95/179 versus 45/134, $P = 9.1 \times 10^{-4}$).

The great majority of the frameshift mutations were clearly heterozygous. Most of the mutations in exon 22 (76/105) were deletions in the A_9 (c.2560delA, one c.2559_2560delAA), nine were deletions in the A_7 (c.2571delA) and two tumours harbored both [c.2560delA(+)c.2571delA]. Additionally, three insertions in the A_9 (c.2560dupA) and one insertion in the G_4 were observed (c.2564dupG). Location of the frameshift mutations and their impact on the C-terminus of the protein is shown in Figure 2A and B. The most frequent mutation (c.2560delA; Figure 1B) in *TTK* extends translation into the 3′ UTR resulting in a peptide that is 34 amino acids longer than the wild-type (Figure 2B). In addition to elongation, three amino acids in the end of the coding region change, one of which (R853G) is probably damaging based on a PolyPhen2 prediction (22).

Fourteen tumours showed ambiguous sequence graphs where two distinct mutant alleles were present in exon 22, typically [c.2560delA(+)c.2571delA]+[c.2560delA]. To investigate whether these tumours could be homozygous (biallelic), laser capture microdissected DNA from two fresh-frozen tumours was amplified and sequenced. Microdissected DNA from both of the tumours revealed the presence of only one mutant allele with wild-type allele, hence no evidence of biallelic mutations was found. A likely explanation for the two mutant alleles is clonal heterogeneity within the tumour cell population. Furthermore, seven MSI tumours had both an NMD-competent mutation (in exon 5 or 2) and an NMD-escaping mutation in exon 22. Cloning and sequencing of individual alleles from amplified cDNA obtained from one tumour revealed that the mutations were in the same allele. Again, no evidence of biallelic mutations was found.

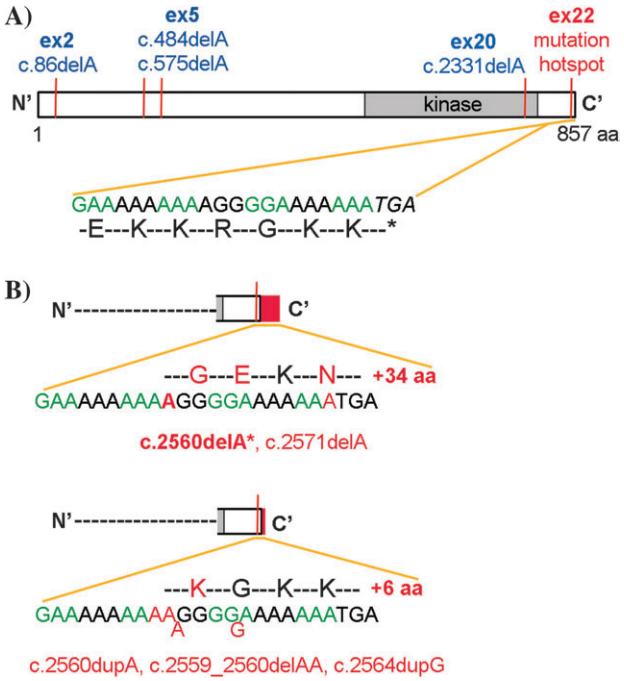

Fig. 2. Location and impact of different *TTK* mutations. The mutation hotspot A_9-G_4-A_7 locates in the end of the coding region in exon 22. (**A**) Truncating mutations found in other exons are shown in blue. Upon c.2560delA (*the most common mutation) or c.2571delA three of the C-terminal amino acids change and the peptide elongates 34 amino acids, which are as follows: DLQLFVMSDTTYKIYWTVILLNPCGNLHLKTTSL. (**B**) Other less common mutations elongate the peptide only six amino acids, specifically: MICSYS. Altered bases and amino acids in the coding region are indicated in red. The R853G change is predicted to be probably damaging according to PolyPhen2 analysis (22).

Clinicopathologic characteristics

Association of *TTK* frameshift mutations with several clinicopathological variables was analyzed altogether in 190 MSI CRCs, of which 11 were obtained from an additional sample series. An association of the mutation with higher histological tumour grade was observed (Table III), and it remained significant after correction for multiple testing ($P = 0.01$). An association with more advanced Duke's stage (Table III) did not remain significant after the correction ($P = 0.15$). No association of the mutation with gender, age at diagnosis or Lynch syndrome germ line mutation was found (Table III). Finally, we examined the association of the *TTK* frameshift mutation with the V600E mutation in its suggested interaction partner, *B-Raf* (23). No association between *B-Raf*^{V600E} and *TTK* mutation in the 100 MSI CRCs analyzed was found (30% had both mutations, $P = 0.85$).

TTK protein in MSI CRC cell lines and primary tumours

A western blot analysis of total protein extracted from six MSI CRC cell lines was performed and clearly showed the presence of the elongated peptide in two mutant cell lines, LoVo and HCT116 (Figure 1C). Only the normal 97 kDa peptide was present in the wild-type VACO5 and HCT8 cell lines, as well as in HCA7 that has a deletion in exon 5. Also, in RKO that has both the exon 5 and 22 deletions, only the normal sized protein was visible, suggesting that these mutations are in the same allele. The amount of the mutant protein in LoVo, and especially in HCT116, appeared to be substantially lower than the wild-type protein. The wild-type protein levels seemed comparable in both the mutant and the wild-type cells.

Likewise, in immunohistochemical staining of TTK, similar subcellular localization and intensity were observed between the heterozygously mutant (n = 5) and wild-type (n = 3) tumours (Figure 1D). Weak to moderate cytoplasmic, and occasionally nuclear, staining was

Table III. Association of *TTK* mutation with clinicopathological features

	Frameshift mutants	Wild-types	*P* value
Male	56	24	0.690
Female	74	36	
Age $\geq$ 69 years	66	33	0.587
Age $<$ 69 years	64	27	
Lynch syndrome mutation	28	10	0.326
No mutation	92	49	
Duke's A–B	83	48	0.030
Duke's C–D	46	12	
Grade I–II	81	51	0.001
Grade III–IV	36	5	

seen in epithelial cells, as well as chromatin staining in mitotic cells. In the normal mucosa, TTK expression seemed to associate with proliferation in the crypt bases, compatible with its function in mitosis.

Subcellular localization of GFP–TTK

TTK is known to be localized to kinetochores in prometaphase cells (24–26). GFP fusions of the wild-type and mutant (c.2560delA) TTK protein were expressed in HEK293 cells in order to determine their subcellular localization. Due to the large amount of diffuse protein, only few prometaphase cells with clear kinetochore localization were found. This was nevertheless comparably observed in both wild-type and mutant-transfected cells (Figure 3A). In interphase cells, the mutant fusion seemed to be aggregating more often in large cytoplasmic vesicles, whereas the expression pattern of the wild-type fusion was more diffused (Figure 3B). The somewhat lower amount of the mutant fusion in comparison with the wild-type (Figure 3C), further suggests that the mutant protein is less well tolerated when ectopically overexpressed. Cell cycle profiles of mutant and wild-type transfected HEK293 cells did not differ according to a flow cytometry analysis (data not shown).

Effect of the microtubule-stabilizing drug paclitaxel on MSI CRC cell lines

The sensitivity of four MSI CRC cell lines to paclitaxel was analyzed with IncuCyte live-cell imaging and colony formation assay. This was performed in order to reveal possible SAC override in the mutated cells and to evaluate their drug sensitivity. LoVo and HCT116 harbor the *TTK* c.2560delA mutation and DLD1 and HCT8 are *TTK* wild-type. These cell lines were cultured with different paclitaxel concentrations and filmed once per hour for 96 h with IncuCyte system. When cultured without the drug (with dimethyl sulfoxide as a negative control), HCT116 and DLD1 grew to become fully confluent and HCT8 reached ~80% confluence (Figure 4A). The growth pattern of LoVo is different and it reached only ~50% confluence even without treatment. When cultured in the presence of 10 nM paclitaxel, a clear reduction in confluence occurred in HCT116 and a smaller reduction in LoVo (Figure 4A). After paclitaxel was added at 21 h, these cells begun to arrest in mitosis and later mostly died from this arrest (Figure 4B; see more time points in supplementary Figure, available at *Carcinogenesis* Online). This suggests that the checkpoint response is functional in the heterozygously mutated cells. On the contrary, the wild-type cells DLD1 and HCT8 showed only minor reduction in confluence (Figure 4A and B) as a result of a transient mitotic arrest, after which the cells escaped from mitosis into the following G_1 phase. With 50 nM concentration, the trend was similar, but the wild-type cells became less confluent (~60 to –70%) compared with 10 nM paclitaxel concentration. The effect of paclitaxel on cellular viability was confirmed with a colony formation assay (Figure 4C), which measures the cells' ability to form progenies irrespective of the mode of cell death. Colony formation in LoVo cells was insufficient for quantification even in control and it was therefore excluded. Viability was reduced by ~20-fold in HCT116 compared with DLD1 and HCT8 already at 5 nM of paclitaxel (Figure 4C).

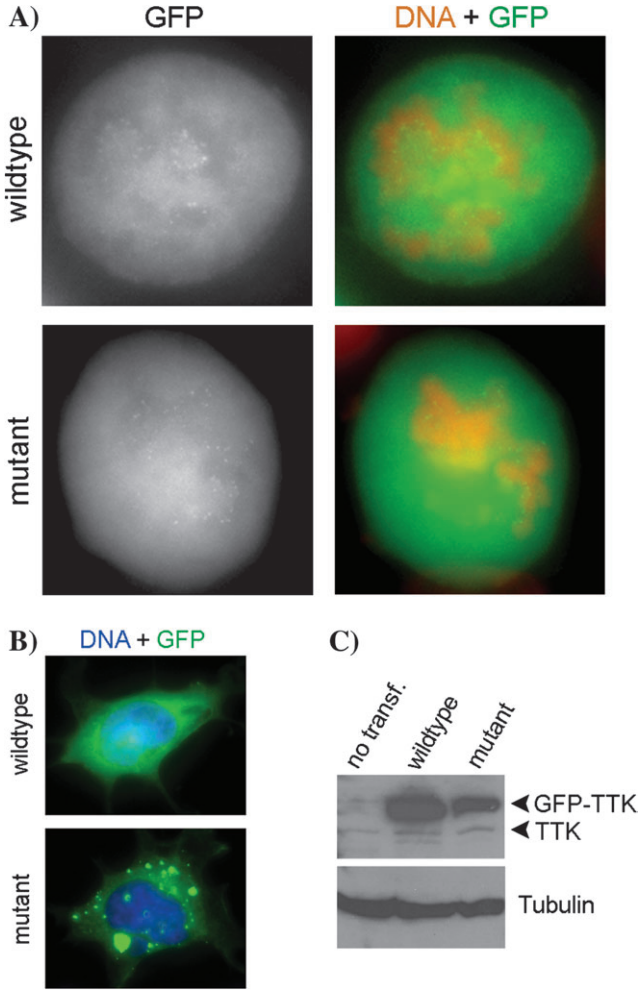

Fig. 3. Subcellular localization of GFP-tagged mutant (c.2560delA) and wild-type TTK. Weak kinetochore accumulation of the GFP fusions in prometaphase HEK293 cells transiently transfected with mutant and wild-type constructs. (**A**) Paclitaxel was added 24 h post-transfection at 20 nM concentration in order to activate the SAC and increase the number of prometaphase cell. Cells were fixed 30 h post-transfection. Large aggregates of GFP fusion were typically seen in the mutant-transfected interphase cells, whereas the wild-type fusion was typically more diffused in the cytoplasm. (**B**) Expression of the GFP fusions in non-treated HEK293 cells 30 h post-transfection (**C**) The mutant fusion was less efficiently expressed in the transfected cells than the wild-type.

Neither mitotic abnormalities nor weakened checkpoint with paclitaxel treatment were observed in HeLa cells transfected with the mutant GFP fusion (data not shown), which strengthens the conclusion that the mutation does not compromise the checkpoint. Attempts to express the mutant and wild-type TTK in MSI CRC cells (with endogenously wild-type *TTK*) caused mainly cell death, which prevented the analysis in an appropriate background.

Discussion

The dual-specificity kinase TTK is involved in the mitotic regulation and signaling in SAC, where it locates at kinetochores and together with other checkpoint components delays anaphase onset until all sister chromatids are correctly attached to microtubules (24,25). In the post-mitotic checkpoint, TTK stabilizes and activates the tumour suppressor p53 in response to spindle damage (27). The kinase is also required for the duplication of centrosomes that serve as microtubule organizing centers in mitosis (28). Microsatellite deletions in the A_9 have previously been reported in 27% (12/44) and 34% (12/35) of

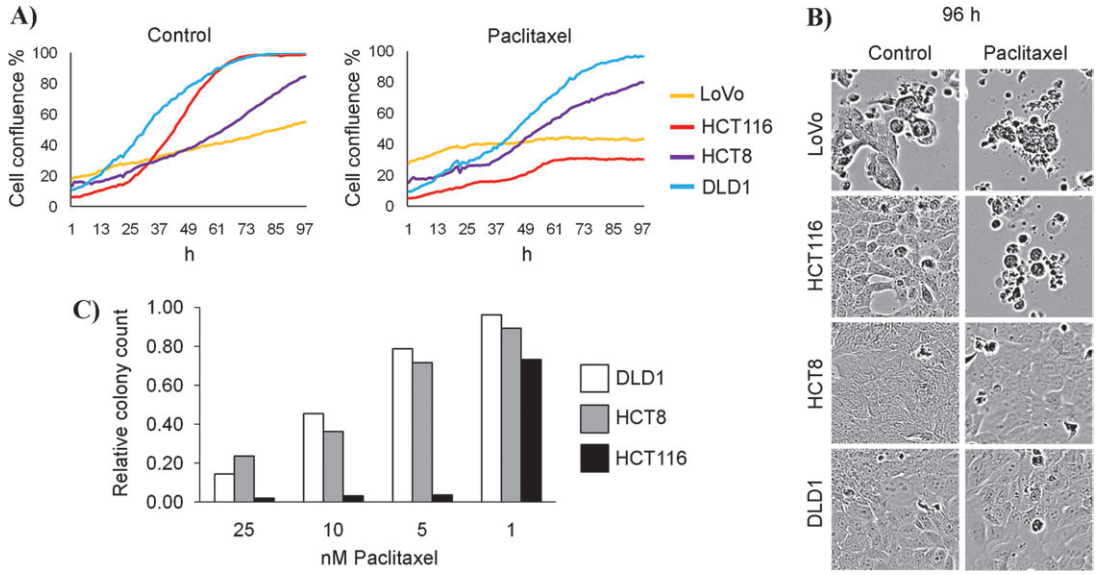

Fig. 4. Cell confluence measured using IncuCyte live-cell imaging in two mutant (LoVo and HCT116) and two wild-type (HCT8 and DLD1) cell lines with 10 nM paclitaxel or with dimethyl sulfoxide as a negative control. (**A**) Paclitaxel was added after 21 h of incubation. Representative details of still images from live-cell imaging at 96 h with or without 10 nM paclitaxel. (**B**) Colony formation capacity (**C**) was drastically reduced in HCT116, compared with DLD1 and HCT8, after paclitaxel treatment (average of two replicate wells). Colony counts in dimethyl sulfoxide-treated controls were set at one and relative counts are shown.

MSI CRCs (29,30). This is much less than what we observed here, which could be due to differences in mutation detection methods. Based on our results, the mutated *TTK* appears to be selected for in the tumourigenesis of MSI CRC since it harbors significantly more mutations under the mismatch repair deficiency than observed in identical control repeats. *TTK* falls among the most highly mutated MSI CRC target genes reported in the literature, such as *TGFBR2* and *ACVR2*, that have been analyzed in a large number of samples (31).

Notably, we were able to show the presence of the 34 residues elongated mutant protein in heterozygous cell lines, confirming its expression. However, lower levels of the mutant than the wild-type protein were detected, indicating that the aberrant mRNA is either controlled by other surveillance mechanisms or that the resulting protein is unstable. Major haploinsufficiency is nonetheless unlikely considering that the wild-type allele in the heterozygously mutated cells seems to produce as much protein as seen in the cells with two wild-type alleles. This is supported by the results of immunohistochemical staining of TTK in primary tumours with and without the mutation. Furthermore, we observed similar subcellular localization of mutant and wild-type GFP fusion in prometaphase cells. This is compatible with previous reports showing that kinetochore localization is mediated by the N-terminus of TTK (26,32) and should therefore not automatically be perturbed by a C-terminal change.

Enrichment of exon 5 mutations in the exon 22 wild-type tumours signals biological significance of the mutations and might indicate that the NMD-competent mutations also give selective advantage. It is possible that complete inactivation of *TTK* is not tolerated in cancer cells. Indeed, no evidence of biallelic mutations was obtained in this study, which could reflect negative selection against them. This is supported by the notion that complete loss of TTK activity causes severe mitotic errors via suppression of other key mitotic kinases such as Aurora B and BubR1, which decreases survival of cancer cells (33–35). However, partial depletion of TTK induces minor chromosome missegregation through weakened SAC leading to aneuploidy, a hallmark of cancer (26,28,34).

Microtubule-stabilizing drugs, such as paclitaxel, hamper normal microtubule dynamics and kinetochore tension that triggers the SAC. Silencing of checkpoint components, including *TTK*, *Bub1B* and *Aurora B* induces both chromosomal instability via reduced mitotic arrest and taxane resistance (14,36). Janssen *et al.* (13) recently reported increased, rather than decreased, sensitivity of *TTK*-silenced cancer cells to paclitaxel, but this was nevertheless caused by reduced mitotic arrest and the resulting chromosome segregation errors. Taxanes have not shown promise in clinical trials of CRC although they are commonly used for several other solid tumours. The reason for this could be the prevalence of chromosomal instability subtype in CRC and hence a compromised SAC function (37,38). Swanton *et al.* (14,37) have suggested that patients with MSI CRC, and presumably intact checkpoint, might actually benefit from taxane treatment. It was therefore relevant to study whether the common *TTK* mutation in MSI CRC affects SAC and taxane response. Here, challenging MSI CRC cell lines with paclitaxel revealed reduced mitotic arrest and less apoptosis, quite surprisingly, in the wild-type cells. Such a difference unlikely depends on the *TTK* mutation but rather on factors related to apoptosis or multidrug resistance. Nonetheless, it seems that a heterozygous *TTK* mutation does not compromise SAC and hence, is not likely to cause slippage from the taxane block. This study provides evidence to support the hypothesis that MSI CRCs are sensitive to taxanes, despite the frequent occurrence of *TTK* mutations.

Until recently, it was unclear whether the unstructured C-terminal tail of TTK has any functional motifs. Interestingly, Sun *et al.* (39) reported that removal of 65 residues from the C-terminus reduced substrate binding and transphosphorylation without affecting autophosphorylation. They also demonstrated that the C-terminus is critical for SAC arrest, but we did not observe SAC override in the cells with c.2560delA mutation that elongates the C-terminus. The functional relevance of the *TTK* frameshift mutation remains to be elucidated. We cannot exclude the possibility that the mutation is merely a neutral bystander event induced by, for instance, flanking sequence properties (40) although the number and distribution of mutations argues for biological significance.

TTK is, nevertheless, involved in several cancer-associated pathways, of which we mainly focused in its most well-established function in the SAC. TTK controls DNA damage responses and genome stability by phosphorylating the Bloom syndrome protein (41), Chk2 in G_2/M checkpoint (42) and the proto-oncogene c-Abl after oxidative stress (43). Lower levels of functional TTK are sufficient for the centrosome duplication than are required for the kinetochore function in SAC (25), which is why the centrosome cycle is unlikely to be dysregulated in the mutant cells. TTK also promotes non-canonical Smad-signaling by phosphorylating Smad2 and Smad3 (44). Furthermore, the oncogenic B-Raf^{V600E} mutant stabilizes TTK through ERK

in human melanomas (22). The *B-Raf*^{V600E} is common in sporadic MSI CRC, but we found no correlation between *B-Raf* and *TTK* mutations.

As a conclusion, heterozygous *TTK* mutations are extremely common in MSI CRCs. The pathogenic nature of the *TTK* mutation has not been analyzed in the previous studies, but Ahn *et al.* (30) reasonably suggested that it might contribute to tumourigenesis by altering cell cycle control. Contrary to expectations, here the mutated cancer cells showed no reduced mitotic arrest after paclitaxel treatment. More work will be needed to scrutinize the effect of *TTK* mutations in other CRC-related biological processes.

Supplementary material

Supplementary information and Figure can be found at http://carcin.oxfordjournals.org/

Funding

Academy of Finland (Center of Excellence in Translational Genome-Scale Biology grant 6302352); the Finnish Cancer Society, the Sigrid Juselius Foundation, the Foundation for the Finnish Cancer Institute and Finnish Graduate School in Computational Sciences; the Research Foundation of the University of Helsinki and the Paulo Foundation to I.N.

Acknowledgements

We thank Sini Nieminen, Sirpa Soisalo, Inga-Lil Svedberg, Iina Vuoristo, Mairi Kuris, Mikko Aho, Maarit Ohranen, Eevi Kaasinen, Yilong Li, Miika Mehine, Jenni Mäki-Jouppila, and Nina Peitsaro for technical assistance.

Conflict of Interest Statement: None declared.

References

1. Aaltonen,L.A. *et al*. (1993) Clues to the pathogenesis of familial colorectal cancer. *Science*, **260**, 812–816.
2. Ionov,Y. *et al*. (1993) Ubiquitous somatic mutations in simple repeated sequences reveal a new mechanism for colonic carcinogenesis. *Nature*, **363**, 558–561.
3. Thibodeau,S.N. *et al*. (1993) Microsatellite instability in cancer of the proximal colon. *Science*, **260**, 816–819.
4. Grady,W.M. (2004) Genomic instability and colon cancer. *Cancer Metastasis Rev.*, **23**, 11–27.
5. Goel,A. *et al*. (2003) Characterization of sporadic colon cancer by patterns of genomic instability. *Cancer Res.*, **63**, 1608–1614.
6. Markowitz,S. *et al*. (1995) Inactivation of the type II TGF-beta receptor in colon cancer cells with microsatellite instability. *Science*, **268**, 1336–1338.
7. Conti,E. *et al*. (2005) Nonsense-mediated mRNA decay: molecular insights and mechanistic variations across species. *Curr. Opin. Cell Biol.*, **17**, 316–325.
8. Nagy,E. *et al*. (1998) A rule for termination-codon position within intron-containing genes: when nonsense affects RNA abundance. *Trends Biochem. Sci.*, **23**, 198–199.
9. El-Bchiri,J. *et al*. (2005) Differential nonsense mediated decay of mutated mRNAs in mismatch repair deficient colorectal cancers. *Hum. Mol. Genet.*, **14**, 2435–2442.
10. Duval,A. *et al*. (2000) The human T-cell transcription factor-4 gene: structure, extensive characterization of alternative splicings, and mutational analysis in colorectal cancer cell lines. *Cancer Res.*, **60**, 3872–3879.
11. Ivanov,I. *et al*. (2007) Identifying candidate colon cancer tumor suppressor genes using inhibition of nonsense-mediated mRNA decay in colon cancer cells. *Oncogene*, **26**, 2873–2884.
12. Miquel,C. *et al*. (2007) Frequent alteration of DNA damage signalling and repair pathways in human colorectal cancers with microsatellite instability. *Oncogene*, **26**, 5919–5926.
13. Janssen,A. *et al*. (2009) Elevating the frequency of chromosome mis-segregation as a strategy to kill tumor cells. *Proc. Natl Acad. Sci. USA*, **106**, 19108–19113.
14. Swanton,C. *et al*. (2007) Regulators of mitotic arrest and ceramide metabolism are determinants of sensitivity to paclitaxel and other chemotherapeutic drugs. *Cancer Cell*, **11**, 498–512.
15. Schmidt,M. *et al*. (2005) Ablation of the spindle assembly checkpoint by a compound targeting Mps1. *EMBO Rep.*, **6**, 866–872.
16. Aaltonen,L.A. *et al*. (1998) Incidence of hereditary nonpolyposis colorectal cancer and the feasibility of molecular screening for the disease. *N. Engl. J. Med.*, **338**, 1481–1487.
17. Salovaara,R. *et al*. (2000) Population-based molecular detection of hereditary nonpolyposis colorectal cancer. *J. Clin. Oncol.*, **18**, 2193–2200.
18. Andersen,C.L. *et al*. (2009) Dysregulation of the transcription factors SOX4, CBFB and SMARCC1 correlates with outcome of colorectal cancer. *Br. J. Cancer*, **100**, 511–523.
19. Pounds,S. *et al*. (2006) Robust estimation of the false discovery rate. *Bioinformatics*, **22**, 1979–1987.
20. Sammalkorpi,H. *et al*. (2007) Background mutation frequency in microsatellite-unstable colorectal cancer. *Cancer Res.*, **67**, 5691–5698.
21. Woerner,S.M. *et al*. (2003) Pathogenesis of DNA repair-deficient cancers: a statistical meta-analysis of putative Real Common Target genes. *Oncogene*, **22**, 2226–2235.
22. Adzhubei,I.A. *et al*. (2010) A method and server for predicting damaging missense mutations. *Nat. Methods*, **7**, 248–249.
23. Cui,Y. *et al*. (2007) B-Raf(V600E) signaling deregulates the mitotic spindle checkpoint through stabilizing Mps1 levels in melanoma cells. *Oncogene*, **27**, 3122–3133.
24. Abrieu,A. *et al*. (2001) Mps1 is a kinetochore-associated kinase essential for the vertebrate mitotic checkpoint. *Cell*, **106**, 83–93.
25. Stucke,V.M. *et al*. (2002) Human Mps1 kinase is required for the spindle assembly checkpoint but not for centrosome duplication. *EMBO J.*, **21**, 1723–1732.
26. Liu,S.T. *et al*. (2003) Human MPS1 kinase is required for mitotic arrest induced by the loss of CENP-E from kinetochores. *Mol. Biol. Cell*, **14**, 1638–1651.
27. Huang,Y.F. *et al*. (2009) TTK/hMps1 mediates the p53-dependent postmitotic checkpoint by phosphorylating p53 at Thr18. *Mol. Cell. Biol.*, **29**, 2935–2944.
28. Fisk,H.A. *et al*. (2003) Human Mps1 protein kinase is required for centrosome duplication and normal mitotic progression. *Proc. Natl Acad. Sci. USA*, **100**, 14875–14880.
29. Mori,Y. *et al*. (2002) Instabilotyping reveals unique mutational spectra in microsatellite-unstable gastric cancers. *Cancer Res.*, **62**, 3641–3645.
30. Ahn,C.H. *et al*. (2009) Mutational analysis of TTK gene in gastric and colorectal cancers with microsatellite instability. *Cancer Res. Treat.*, **41**, 224–228.
31. Woerner,S.M. *et al*. (2006) Microsatellite instability in the development of DNA mismatch repair deficient tumors. *Cancer Biomarkers*, **2**, 69–86.
32. Stucke,V.M. *et al*. (2004) Kinetochore localization and microtubule interaction of the human spindle checkpoint kinase Mps1. *Chromosoma*, **113**, 1–15.
33. Huang,H. *et al*. (2008) Phosphorylation sites in BubR1 that regulate kinetochore attachment, tension, and mitotic exit. *J. Cell Biol.*, **183**, 667–680.
34. Jelluma,N. *et al*. (2008) Chromosomal instability by inefficient Mps1 autoactivation due to a weakened mitotic checkpoint and lagging chromosomes. *PLoS One*, **3**, e2415.
35. Jelluma,N. *et al*. (2008) Mps1 phosphorylates Borealin to control Aurora B activity and chromosome alignment. *Cell*, **132**, 233–246.
36. Schliekelman,M. *et al*. (2009) Impaired Bub1 function in vivo compromises tension-dependent checkpoint function leading to aneuploidy and tumorigenesis. *Cancer Res.*, **69**, 45–54.
37. Swanton,C. *et al*. (2006) Chromosomal instability, colorectal cancer and taxane resistance. *Cell Cycle*, **5**, 818–823.
38. Swanton,C. *et al*. (2009) Chromosomal instability determines taxane response. *Proc. Natl Acad. Sci. USA*, **106**, 8671–8676.
39. Sun,T. *et al*. (2010) Cellular abundance of Mps1 and the role of its carboxyl terminal tail in substrate recruitment. *J. Biol. Chem.*
40. Chung,H. *et al*. (2010) Flanking sequence specificity determines coding microsatellite heteroduplex and mutation rates with defective DNA mismatch repair (MMR). *Oncogene*, **29**, 2172–2180.
41. Leng,M. *et al*. (2006) MPS1-dependent mitotic BLM phosphorylation is important for chromosome stability. *Proc. Natl Acad. Sci. USA*, **103**, 11485–11490.
42. Wei,J.H. *et al*. (2005) TTK/hMps1 participates in the regulation of DNA damage checkpoint response by phosphorylating CHK2 on threonine 68. *J. Biol. Chem.*, **280**, 7748–7757.
43. Nihira,K. *et al*. (2008) TTK/Mps1 controls nuclear targeting of c-Abl by 14-3-3-coupled phosphorylation in response to oxidative stress. *Oncogene*, **27**, 7285–7295.
44. Zhu,S. *et al*. (2007) Activation of Mps1 promotes transforming growth factor-beta-independent Smad signaling. *J. Biol. Chem.*, **282**, 18327–18338.

Received July 13, 2010; revised November 26, 2010; accepted December 11, 2010